RESEARCH ARTICLE

Methanol synthesis at a wide range of H_2/CO_2 ratios over Rh-In bimetallic catalyst

Molly Meng-Jung Li[†], Hanbo Zou[†], Jianwei Zheng[†], Tai-Sing Wu, Ting-Shan Chan, Yun-Liang Soo, Xin-Ping Wu, Xue-Qing Gong, Tianyi Chen, Kanak Roy, Georg Held, Shik Chi Edman Tsang*

Abstract: Recent years have seen an increasing interest in capturing hydrogen generated from renewables with CO_2 to produce methanol. However, renewable hydrogen production is currently expensive and in limited quantity as compared to CO_2. Excess CO_2 and limited H_2 in the feedstock gas mixture is not favourable for the CO_2 hydrogenation to methanol reaction, which causes low activity and poor methanol selectivity. Here we report a new class of Rh-In catalysts with optimal adsorption property to the intermediates of methanol production. The Rh-In catalyst can effectively catalyse methanol synthesis but inhibit reverse water-gas shift reaction under H_2-deficient gas flow and shows the best competitive methanol productivity under industrially applicable conditions in comparison with the literature reported values. This work demonstrates a strong potential of Rh-In bimetallic composition, from which a convenient methanol synthesis based on flexible feedstock compositions (e.g. H_2/CO_2 from biomass derivatives) with lower energy cost can be established.

Introduction

Hydrogen always plays a critical role as an energy vector in human activity despite the fact that there is almost no free form of naturally occurring hydrogen on earth. At present, most of the world's hydrogen is derived from carbon-containing fossil fuels, its utilisation leads to concomitantly a huge surge in carbon emission to the atmosphere. On the other hand, hydrogen can also be produced from electrolysis of water using renewable energy such as solar energy, wind power, hydropower, ground heat, or biomass.[1] When hydrogen is combusted or used in a fuel cell elsewhere, the major by-product is water again, thus completing the truly circular economy with energy storage and dispatch with no greenhouse gas emission. Although the current low water splitting efficiency does not yet justify for the massive launch of this technology, the progressive improvement in electrolyser, special locations with particular availability of renewable energy sources, and increasing carbon taxation make this new process attractive. For safe and efficient transport of hydrogen energy at long distance, suitable organic hydrogen carriers are under extensive investigations. From an economic perspective, methanol shows high potential as a hydrogen carrier.[2] Therefore, recent years have seen an increasing interest in storing renewable hydrogen by reacting it with CO_2 to form green methanol and reverse the process to reobtain the H_2.[3] In addition, catalytic aqueous-phase reforming (APR) is regarded as a promising technology for production of renewable hydrogen (if the reaction is powered by renewable energy sources) and soluble chemicals from biomass-derived substances in aqueous phase under elevated pressure and temperature. It can result in the formation of hydrogen and CO_2 as the main products in the gas phase from fragile biomass-derived substances, providing suitable feedstock mixtures for CO_2 hydrogenation to methanol hence creating a good opportunity for the effective valorisation of waste biomass to fuel and chemicals.[4] However, the direct utilisation of biomass for methanol production faces the problem of a large excess CO_2 in the reforming gas mixture ($H_2/CO_2 < 3$). Therefore, the stoichiometric adjustment has to be applied either by adding hydrogen or removing CO_2, which requires burdensome equipment and high costs.[5,6] Similarly, the production of hydrogen from other renewable means is rather expensive and is produced in limited quantity as compared to CO_2 capture.[7] As a result, an effective catalyst to seize hydrogen in the CO_2-excess/H_2-deficient conditions to catalyse CO_2 hydrogenation to methanol would be highly desirable.

It is known that bimetallic nanoparticles/alloys with intimate contacts of the two elements can modify the electronic properties of the constituent metals, thus change their adsorption properties.[8,9] A good example can be found in the Cu-Zn system, which shows that the Zn-modified Cu surface gives better methanol production rates than the unmodified Cu surface because the Zn-modified Cu surface has a stronger binding of intermediates and lower energetic barriers to the methanol product.[10–12] Although the adsorption property of the Cu surface can be improved by modifying with Zn species, the Cu surface still possesses the drawbacks on the low activity for hydrogen activation, which leads to low coverage of surface H and slows down the further hydrogenation of the intermediates into methanol.[8] Consequently, for the Cu-based catalysts, high methanol selectivity commonly requires an extreme reaction condition (high pressure of over 10 MPa, high ratios of $H_2:CO_2 \geq 3$), otherwise CO is favourably produced through the reverse water-gas shift reaction (RWGS) route.[13] In addition, it has been reported that methanol selectivity of the Cu-based catalysts is limited according to thermodynamic calculations,[8] which leads to significant CO production through the RWGS. Therefore, non-Cu

[*] Dr. M. M.-J Li[†], Dr. H. Zou[†], Dr. J. Zheng[†], T. Chen, Prof. S. C. E. Tsang*
Department of Chemistry, University of Oxford, OX1 3QR, UK.
E-mail: edman.tsang@chem.ox.ac.uk
Dr. H. Zou
Department of Chemistry and Chemical Engineering, Guangzhou University, China.
Dr. T.-S. Wu, Prof. Y.-L. Soo
National Synchrotron Radiation Research Center, Hsinchu, Taiwan.
and
Department of Physics, National Tsing Hua University, Hsinchu, Taiwan.
Dr. T.-S. Chan
National Synchrotron Radiation Research Center, Hsinchu, Taiwan.
Dr. X.-P. Wu, Prof. X.-Q. Gong
Key Laboratory for Advanced Materials, Centre for Computational Chemistry and Research Institute of Industrial Catalysis, East China University of Science and Technology, Shanghai 200237, People's Republic of China
Dr. K. Roy, Prof. G. Held
Diamond Light Source, Harwell Campus, Chilton, Oxfordshire OX11 0DE, UK
[†] These authors contributed equally to this work.
Supporting information for this article is given via a link at the end of the document.

based catalysts for effectively utilising renewable hydrogen from renewables-derived feedstocks (e.g. biomass) to green methanol production are needed to accomplish this development.

Here we report a novel Rh-In bimetallic catalyst *for the first time* that shows very effective usage of H_2 toward methanol production. Rh-In bimetallic catalyst not only shows the best competitive methanol productivity per gram basis under industrially applicable conditions in comparison with the literature-reported values but also maintains high H_2 conversion to methanol under H_2-deficient gas flow. This new catalyst displays its advantages in efficient H_2 utilisation with the undesired RWGS reaction, i.e. CO production, being minimised under flexible feedstock compositions.

Results and Discussion

In this study, a series of Rh-containing samples with different In/Al compositions have been synthesised (see Table 1 for sample names and preparation details) and assessed in the CO_2 hydrogenation reaction. As can be seen from Fig. 1a, at the same reaction temperature of 270 °C, the wet-impregnation samples with In/Al ratios from 0 to 1 give a diverse product composition: The sample contains no In (im-Rh/Al_2O_3) shows a total conversion of CO_2 to methane, while CO is predominant in the product composition when im-RhIn/(1In9Al)O is used. Methanol initially emerges in im-RhIn/(1In9Al)O and becomes substantial (>85% selectivity) in im-RhIn/(5In5Al)O and im-RhIn/In_2O_3. For the typical partial reduction reaction like CO_2 hydrogenation to methanol instead of CH_4, methanol selectivity normally has an inverse relationship with CO_2 conversion. Therefore the catalysts were also assessed and compared under the same CO_2 conversion of 1%, where kinetic plug-flow conditions (far from equilibrium) are ensured. The result in Fig. 1b shows the same trend of increasing methanol selectivity as In concentration increases: Methanol selectivity is peaked at the im-RhIn(5In5Al)O catalyst and then starts to decrease. These results suggest that In/Al=1 is the optimal support composition for the Rh catalysts, and the presence of In near Rh can significantly alter the catalytic properties of Rh sites from methanation (In/Al=0) toward RWGS reaction (In/Al=1/9), and finally to methanol production (In/Al>1). Such an effective modification of Rh has not been reported in the literature. Although, when doping with alkaline earth metals[14] or alloying with Co,[15] Rh-based catalysts can have a slight enhancement on CO/CO_2 hydrogenation to methanol. However, the yield and selectivity toward methanol production in those early works were much lower than the In-modified Rh catalysts in our study. On the other hand, the In_2O_3-Al_2O_3 sample only gives 30% methanol selectivity with a low CO_2 conversion under the same testing condition (Fig. 1a&b). This indicates that In_2O_3 does not contribute to high methanol production due to its limited H_2-splitting ability.[16] An In-modified Ru counterpart, im-Ru/(5In5Al)O, has also been evaluated (Fig. 1c). Although the increases in methanol selectivities can be observed upon adding In into Ru/Al_2O_3 catalyst, the methanation of CO_2 over the im-Ru/(5In5Al)O sample cannot be excluded as a noticeable amount of methane still appears in its product composition, especially at a higher reaction temperature of 330 °C. This suggests that the In

modification to Ru sites is not as effective as the Rh sites, which could be attributed to the ineffective d-band modification of the electron poorer Ru by In to alter their intrinsically strong adsorptive and catalytic properties. Alternatively, In modification to Ru may be extensively carried out using other synthesis processes to increase the interactions between Ru and In species to improve its effectiveness. This requires more experimental studies.

It is noted that CO_2 conversion drops drastically when incorporating In into Rh (Fig. 1a), however, a decent CO_2 conversion (>10%) can be achieved when using In-modified Rh catalyst prepared by the co-precipitation method, denoted as co-RhIn/(5In5Al)O (see Fig. 1c). The specific surface areas (3.2 ± 0.1 m^2g^{-1} for im-RhIn/(5In5Al)O and 279.5 ± 0.2 m^2g^{-1} for co-RhIn/(5In5Al)O) determined by BET as well as the Rh surface areas (17.3 $m^2g_{-Rh}^{-1}$ for im-RhIn/(5In5Al)O and 132.6 $m^2g_{-Rh}^{-1}$ for co-RhIn/(5In5Al)O) determined by hydrogen/oxygen titration reveal that the co-precipitation method can increase the surface exposure of Rh. TEM images and particle size distribution diagrams (Fig. S3) also suggest that the metal nanoparticles prepared by the co-precipitation method indeed have a significantly smaller particle size (1 ~ 5 nm) compared to the wet-impregnation sample (>20 nm). In correlation with the catalytic performance (Fig. 1c), both im-RhIn/(5In5Al)O and co-RhIn/(5In5Al)O catalysts show a good selectivity to methanol. However, the activity of im-RhIn/(5In5Al)O is much lower. The larger particle size of im-RhIn/(5In5Al)O can reduce the number of the exposed active sites, therefore causing a lower CO_2 conversion. Note that methanol selectivity does not change along with the metal particle size variation, implying that selectivity is not critically size-dependent in this In-modified Rh catalyst system.

Fig. 1d shows methanol selectivities of the best-performing catalyst, co-RhIn/(5In5Al)O, assessed in CO_2 hydrogenation with different CO_2/H_2 ratios (from 1/3 to 3). A commercial $Cu/ZnO/Al_2O_3$ catalyst is also evaluated for the comparison. In CO_2 hydrogenation reaction to methanol, the use of gas mixture with $H_2/CO_2 < 3$ is not thermodynamically favourable. Understandably, the practical methanol selectivities obtained on the $Cu/ZnO/Al_2O_3$ catalyst continuously drop when increasing CO_2/H_2 ratios from 1/3 to 3. Fig. S5a shows that the methanol yields from both co-RhIn/(5In5Al)O and $Cu/ZnO/Al_2O_3$ catalysts are lower than the calculated thermodynamic equilibrium values with unconverted reactants when taken both methanol production and RWGS equilibria into account. The data clearly imply that the catalysed reaction is under kinetic control. However, for the co-RhIn/(5In5Al)O catalyst, especially at the excess CO_2 conditions, methanol selectivities remain at higher values, which are even higher than the thermodynamic predicted selectivities, assuming both methanol production and RWGS reached equilibria (indicated by the dashed/dotted lines in Fig. 1d). Note that co-RhIn/(5In5Al)O can attain higher methanol yields than that of thermodynamic prediction from CO_2 to methanol and RWGS when H_2/CO_2 is lower than 0.5 (H_2-deficient). These results suggest that the RWGS reaction can be effectively suppressed on the In-modified Rh catalyst, particularly under low H_2/CO_2 conditions, hence minimising CO production on this catalyst (details will be discussed later along with the DFT calculation). Considering that H_2 is more valuable than CO_2, minimising H_2 consumption in producing unwanted products (i.e. CH_4, H_2O, etc.)

is very important. Fig. 1e presents the H_2 conversion (added up by the H_2 consumptions in methanol production and the RWGS reaction) of both co-RhIn/(5In5Al)O and Cu/ZnO/Al$_2$O$_3$. Although Cu/ZnO/Al$_2$O$_3$ shows a slightly higher H_2 conversion than co-RhIn/(5In5Al)O, its majority of H_2 conversion is attributed to RWGS reaction, that produces CO and H_2O. On the other hand, co-RhIn/(5In5Al)O shows a very efficient usage of H_2 toward methanol production, and it can maintain high H_2 conversion to methanol even under H_2-deficient conditions (H_2/CO$_2$ < 3). This result has proven that co-RhIn/(5In5Al)O catalyst can efficiently seize hydrogen in the H_2-deficient environment and selectively catalyse CO_2 hydrogenation to methanol without consuming a large quantity of valuable H_2 on the RWGS reaction.

Fig. 1f gives the methanol space-time yields (STY, g$_{MeOH}$·g$_{cat}^{-1}$·h^{-1}) and methanol selectivities of co-RhIn/(5In5Al) and Cu/ZnO/Al$_2$O$_3$. Noticeably, the methanol selectivity and STY of Cu/ZnO/Al$_2$O$_3$ are significantly less than those of co-RhIn/(5In5Al). Moreover, methanol selectivity and STY of co-RhIn/(5In5Al) can be further optimised by adjusting the weight hourly space velocity (WHSV) to reach nearly 100% and over 1.0 g$_{MeOH}$·g$_{cat}^{-1}$·h^{-1}, respectively. As far as we are aware, STY of 1.0 g$_{MeOH}$·g$_{cat}^{-1}$·h^{-1} obtained by co-RhIn/(5In5Al)O at CO$_2$/H$_2$ = 1/3 condition is among the highest values compared to the state-of-the-art catalysts in the literature.[8,9,16–28] The comparison of co-RhIn/(5In5Al) to the traditional Cu-based catalysts and the state-of-the-art catalysts is presented in Section 4 of the supporting information (SI) and Table S1.

Time-on-stream (TOS) test was also performed to evaluate the stability of the co-RhIn/(5In5Al) catalyst. Fig.S5b shows that co-RhIn/(5In5Al)O gives consistently high methanol selectivity and CO$_2$ conversion for at least 10 days in our academic laboratory reactor. Although a longer TOS test should be vigorously studied at a large scale to determine its suitability for industrial applications, the Rh-In catalyst appears to be stable during the CO$_2$ hydrogenation test in our laboratory.

Table 1 The details of the synthesis method, metal loading, and In/Al ratio of all catalysts presented in this work.

Sample name	Rh or Ru loading & method	In : Al ratio of In$_2$O$_3$-Al$_2$O$_3$ support
im-Rh/Al$_2$O$_3$	5%, wet-impregnation	0 : 10
im-RhIn/(1In9Al)O	5%, wet-impregnation	1 : 9
im-RhIn/(3In7Al)O	5%, wet-impregnation	3 : 7
im-RhIn/(5In5Al)O	5%, wet-impregnation	5 : 5
im-RhIn/In$_2$O$_3$	5%, wet-impregnation	10 : 0
In$_2$O$_3$-Al$_2$O$_3$	No Rh loading	5 : 5
im-Ru/(5In5Al)O	5%, wet-impregnation	5 : 5
co-RhIn/(5In5Al)O	2.5%, co-precipitation	5 : 5
co-Rh/Al$_2$O$_3$	2.5%, co-precipitation	0 : 10
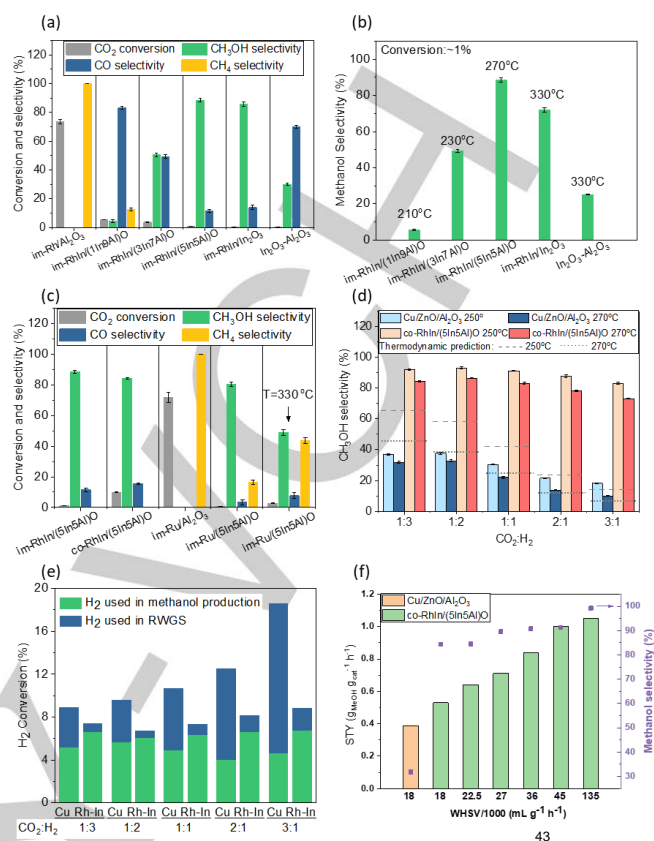
Figure 1. Catalytic performance of CO$_2$ hydrogenation to methanol. Typical testing conditions are the pressure of 45 bar, reactant mixture of CO$_2$/H$_2$=1/3, reaction temperature of 270 ºC, WHSV of 18000 mL g^{-1} h^{-1} unless otherwise indicated. Error bars in the figures indicate the standard deviation of at least 3 repeated data points taken for each experiment. a) CO$_2$ conversions and the selectivities of CO, CH$_3$OH, and CH$_4$ of Rh catalysts with different In/Al ratios prepared via the wet-impregnation method. b) Methanol selectivities of Rh catalysts prepared by wet-impregnation methods when evaluated under the same CO$_2$ conversion of 1% (with the typical standard deviations lower than 0.1%). Reaction temperatures to achieve 1% CO$_2$ conversion are stated for each catalyst. c) CO$_2$ conversions and the selectivities of CO, CH$_3$OH, and CH$_4$ of Rh and Ru catalysts with different In/Al ratios prepared via wet-impregnation and co-precipitation methods. d) Methanol selectivities at 250 ºC and 270 ºC of co-RhIn/(5In5Al)O sample compared with the commercial Cu/ZnO/Al$_2$O$_3$ catalyst under different CO$_2$/H$_2$ ratios. The dashed/dotted lines indicate the calculated methanol selectivities by taking both methanol synthesis and RWGS equilibria into account. The decreasing trend for both catalysts is according to the thermodynamic limits when a higher CO$_2$/H$_2$ ratio is employed. e) H$_2$ conversion toward methanol production (green) and RWGS reaction (blue) of co-RhIn/(5In5Al)O compared with Cu/ZnO/Al$_2$O$_3$ catalyst under different CO$_2$/H$_2$ ratios. f) Methanol space-time yields and selectivities of co-RhIn/(5In5Al)O and Cu/ZnO/Al$_2$O$_3$ under different WHSV.

To realise the impact of In addition to Rh catalysts, the structural investigation was conducted. From TEM images in Fig. S3, we can see that the reduced co-Rh/Al$_2$O$_3$ has a similar but slightly smaller Rh containing particle size than the reduced co-RhIn/(5In5Al)O. BET analysis of these two samples shows that both have high surface areas (279.5 m²/g for co-RhIn/(5In5Al)O and 327.8 ± 0.5 m²/g for co-Rh/Al$_2$O$_3$). These results imply that In addition does not have a huge impact on the size of Rh nanoparticles but its presence can significantly alter the product

composition of CO_2 hydrogenation, hence the change of catalytic performance upon varying In/Al ratio is not originated from Rh size variation. HR-TEM images in Fig. 2a and Fig. S4a reveal that small islands of the two most stable crystalline intermediate phases of the Rh-In system (cubic-RhIn and tetragonal-$RhIn_3$) at the material interfaces were observed.[29] TEM of the co-RhIn/(5In5Al)O catalyst retrieved at the end of the long TOS test also shows that both cubic-RhIn and tetragonal-$RhIn_3$ clusters embedded with the variable $RhIn_x$ composition at the metal-support interfaces with no observable particle sintering in the post-reaction catalyst (Fig. S4b), suggesting that Rh-In alloys are robust to maintain throughout the CO_2 hydrogenation mixture. On the other hand, the main light-contrast particles in the vicinity of darker Rh-In alloy clusters in the TEM images are confirmed to be hexagonal In_2O_3 (Fig. S4 a&b). This observation is in agreement with the XRD patterns in Fig. S4c that the hexagonal In_2O_3 phase is the predominant structure in the co-RhIn/(5In5Al)O sample either before or after catalytic CO_2 hydrogenation testing. We cannot detect any Rh-containing phases from XRD patterns due to either the low Rh metal loading (~2.5 wt.%) or the diffraction-line broadening caused by small particle sizes, and the absence of aluminium oxide phase indicates that it is amorphous in nature.

Analysis of the EXAFS at both Rh and In K-edge was employed to provide detailed information on the local atomic structure of Rh and In atoms. Fig. 2b shows Fourier-transform Rh K-edge EXAFS of the reduced Rh-containing catalysts. The k^3-weighted EXAFS (K space) with the corresponding fittings are shown in Fig. S6, and the fitting parameters are detailed in Table S2. It can be seen from Fig. 2b that in general, each Rh-containing sample has two main shells, that is, an Rh-O shell at around 2Å and the Rh-metal shell at the longer distance. Since all the samples were pre-reduced in H_2 and carefully handled in oxygen-free conditions prior to the XAS measurements, the Rh-O scattering path detected in EXAFS spectra is most likely attributed to the interaction between Rh and the oxygen from the oxide support. For the im-Rh/Al_2O_3 sample, the observed Rh-O peak is higher than the Rh-Rh bond, indicating that Rh nanoparticles have strong interaction with the Al_2O_3 support. As In concentration increases, the coordination number (C.N.) of Rh-O decreases as well as the distance of the Rh-Rh scattering path at around 2.66-2.70 Å increases, suggesting a weakening interaction between Rh atoms and the oxide support while strengthening the interaction between Rh and the neighbouring In species. Besides, in the EXAFS spectra of the catalysts with the optimal support composition (In/Al=1), i.e., im-RhIn/(5In5Al)O and co-RhIn/(5In5Al)O, there are three distinctive scattering paths observed at the distances of 2.64, 2.82 and 3.07 Å, that are attributed to Rh-In, Rh-In and Rh-Rh bonds, respectively, evidencing the formation of Rh-In alloy structure. The im-RhIn/In_2O_3 sample gives the highest Rh-In alloy content among all the Rh-containing samples due to its highest C.N. of Rh-In scattering paths. Besides, im-RhIn/In_2O_3 contains no Rh-O, showing the fact that the interaction between Rh and the oxygen from In_2O_3 is negligible.

Fig. 2c gives H_2-TPR profiles of the Rh-containing catalysts and the In_2O_3-Al_2O_3 catalyst. For the im-Rh/Al_2O_3 sample, the reduction peaks at 135 and 248 °C are attributed to the well-dispersed surface Rh_2O_3 and the bulk-like/crystalline Rh_2O_3 particles, respectively,[30] According to the published data, the high-temperature TPR peak may also stem from the strong interaction of Rh species with the Al_2O_3 support.[31] As In concentration increases, (from In/Al=0 to In/Al=3/7), the low-temperature Rh reduction peak increases with the disappearance of the high-temperature reduction peak, indicating the interaction between Rh and Al_2O_3 support has been diminished, similar to what was observed in the Rh K-edge EXAFS analysis. Interestingly, for the catalysts having a composition of In/Al ≥ 1, the Rh reduction peak flattens and shifts to a higher temperature, which is indicative of the increased metal-metal interaction of Rh and In when In concentration has increased.[31]
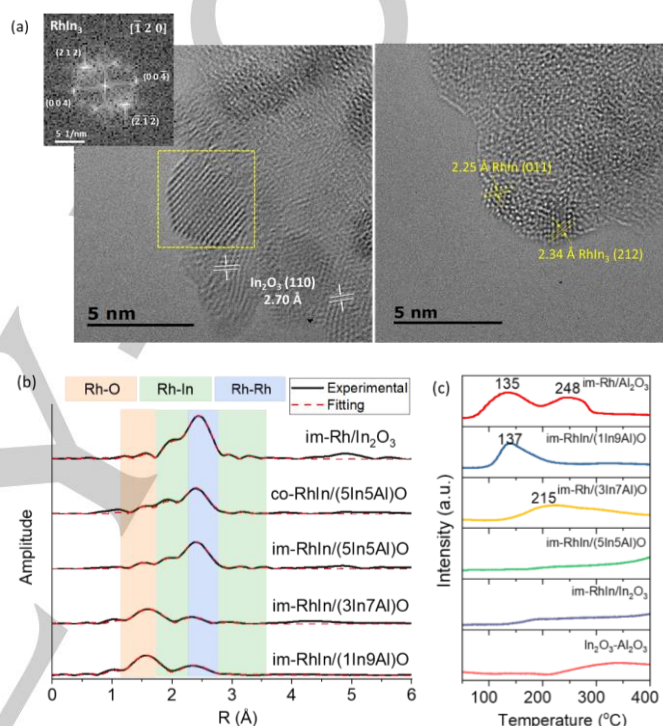
Figure 2. Structure and the reduction behavior
a) HR-TEM images with the fast-Fourier Transform (FFT) analyses of the selected Rh-In alloy nanoparticles and the measured d-spacings corresponding to the hexagonal In_2O_3 phase in the freshly reduced co-RhIn/(5In5Al)O catalyst. b) k^3-weighted Rh K-edge EXAFS Fourier transforms of the reduced Rh and In-modified Rh samples. c) H_2-TPR profiles of the Rh, In-modified Rh catalysts, and In_2O_3-Al_2O_3 support.

The electronic properties of the catalysts were also investigated using XANES and XPS. Rh K-edge XANES spectra (Fig. 3a) reveal that the catalysts containing the support compositions of In/Al ≥ 1 have similar Rh absorption edges that are comparable to the absorption edge of Rh foil. As for the samples with less In concentrations (In/Al < 1), their Rh absorption edge positions progressively shift toward high energy along with the decrease of In/Al, which is indicative of higher oxidation state of Rh. A similar trend of binding energy shift can also be observed from Rh *3d* XPS spectra (Fig. 3b). This again reveals that the interaction between Rh and oxygen from the oxide support could be minimised upon In incorporation. Besides, the alteration of the electronic property of Rh also signifies that charge transfer can occur from In to Rh when forming Rh-In alloy,

which is in agreement with the thermodynamic observation reported in the literature.[29] In contrast, In 3d XPS spectra (Fig. 3b) of the reduced samples show no distinguishable shift upon In incorporating into Rh catalysts due to the fact that most In species stay as oxidic and only limited In_2O_3 reduction could prompt the decoration of In on Rh, as confirmed by XRD (Fig. S4c) and In L_3-edge XANES (Fig. S6b) showing that In mainly retains as the In_2O_3 phase no matter before or after CO_2 hydrogenation reaction.

Synchrotron-based near ambient-pressure X-ray photoelectron spectroscopy (NAP-XPS) was then employed to study the in-situ change of the chemical states in the co-RhIn/(5In5Al)O under catalytic working conditions. Fig. 3c shows Rh 3d and In 3d NAP-XPS spectra recorded in situ during Ar, H_2, and CO_2/H_2 atmospheres at 290 °C. Our experimental determined binding energies (BE) of Rh $3d_{5/2}$ peaks are comparable to the published data (Rh^{3+} $3d_{5/2}$ = 308.4, Rh^0 $3d_{5/2}$ = 307.2).[32] The Rh 3d spectra (i) and (ii) provide a clear indication of the rapid and complete Rh^{3+} reduction to form Rh^0. From spectra (ii) to (iv), the Rh $3d_{5/2}$ BE keeps decreasing beyond the metallic Rh^0 $3d_{5/2}$ value (307.4 eV) with further exposure to H_2 for a longer period of time, which indicates that the Rh species become electron richer. As for the In 3d NAP-XPS spectra, two $3d_{5/2}$ and two $3d_{3/2}$ peaks can be found in each spectrum taken under different gas conditions. According to the literature, BE of In^{3+} $3d_{5/2}$ is around 444.8 eV, whereas BE of In^0 $3d_{5/2}$ is ranging from 442.8 to 443.7 eV. [33,34] Our experimentally determined In 3d region shows two sets of the well-separated $3d_{5/2}$ and $3d_{3/2}$ orbitals both having the typical energy difference of spin-orbit components (Δ=7.6 eV) of In. In addition, their BEs match the literature-reported values of metallic In and oxidised In species. As a result, the $3d_{5/2}$ and $3d_{3/2}$ peaks at lower BEs (ca. 443 eV and 450 eV, respectively) can be identified as metallic In while the higher-BE In $3d_{5/2}$ and $3d_{3/2}$ peaks (ca. 445 eV and 452.6 eV, respectively) are attributed to In_2O_3. From spectrum (i), it can be seen that In shows some degree of reduction due to the high-temperature treatment in Ar atmosphere. When the gas feed is changed to H_2, the In^0 $3d_{5/2}$ signal starts to increase and shifts slightly to higher BE (from 442.6 to 442.9 eV), which falls simultaneously in line with the shift of Rh^0 $3d_{5/2}$ to lower BE. This offers the evidence of charge transfer from In to Rh due to the formation of local alloys at the materials' interfaces. In the 2nd H_2 exposure, we can see from spectrum (iii) that the intensity of In^0 $3d_{5/2}$ peak further increases with its BE shifting to 443.3 eV. This clearly suggests that the prolonged H_2 exposure will result in a deeper reduction of support so that more In^0 species can react with the vicinity Rh^0 to form more extensively In-decorated Rh, leading to two stable Rh-In alloy phases observed. In the 3rd H_2 exposure, see spectrum (iv), In^0 $3d_{5/2}$ signal stays unchanged compared with spectrum (iii), suggesting the establishment of stable Rh-In alloys at the interface. When switching the H_2 gas to CO_2/H_2, In^0 $3d_{5/2}$ signal still exists but the intensity decreases with the reduction of BE, suggesting that CO_2 in the reaction mixture can act as an oxidant to gently oxidise Rh-In alloys.
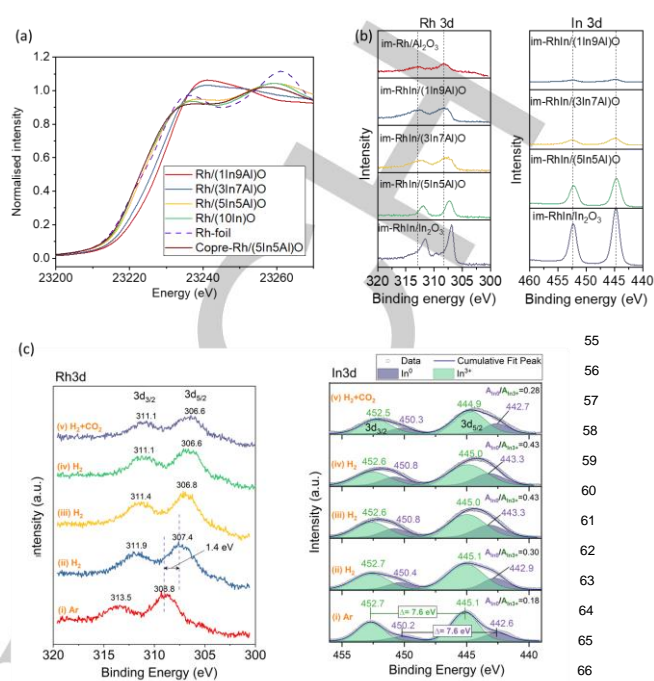
Figure 3. Electronic structure of the Rh-In catalyst a) Normalised Rh K-edge XANES spectra and b) XPS Rh 3d and In 3d spectra of the reduced Rh and In-modified Rh samples. c) NAP-XPS of Rh 3d and In 3d as a function of different gas atmospheres at 290 °C.

It is well-known that the foreign metal atom additives/impurities in metal catalysts can induce the formation of bimetallic nanoparticles/alloys, which would significantly modify the electronic configurations hence altering the adsorption properties of the original metal sites and dictating product specificity. Many examples have been recently reported including the Cu-Zn,[10–12] Pd-Zn,[8,9] Pd-Ga, Pd-In,[35] Ni-Ga[18] bimetallic catalysts for the enhanced CO/CO_2 hydrogenation to methanol. According to theoretical calculations,[18,36–39] catalytic activity of CO_2 hydrogenation to methanol is critically dependent on the overall adsorptivity of catalytic surfaces. In earlier studies on the reaction pathways of CO_2 hydrogenation to methanol, there are two proposed parallel pathways: One is through a formate (HCOO*) intermediate without CO formation; the other involves a hydrocarboxyl (COOH*) intermediate, through which CO_2 is first converted to CO (RWGS route) and then CO can be further hydrogenated to methanol.[40,41] The catalytic performance and the intermediates formed during reactions have been demonstrated to be dependent and sensitive to the composition of catalysts. For the industrial $Cu/ZnO/Al_2O_3$ catalyst composition, the formation of electron richer metal, i.e. Zn, tends to stabilise more to the formate intermediate, however, the role(s) and interactions of each component in this catalyst are still in debate.[10,42]

Density functional theory (DFT) calculations were therefore carried out to simulate the change of adsorption property of Rh surface upon incorporating In species from the local In_2O_3 reduction. To be more specific, the competitive routes of HCOO*

and COOH* on Rh and bimetallic Rh-In surfaces will be appreciated and compared with the Cu-Zn surfaces symbolic of the commercial Cu/ZnO/Al₂O₃ catalyst. The effect of In₂O₃-Al₂O₃ support was not considered in our DFT calculations as our experimental results clearly show that the support does not contribute to high methanol production. In contrast, the bimetallic nature of the catalyst and the strong synergy between bimetallic Rh and In presented in the above X-ray spectroscopic analysis are believed to contribute to the unprecedentedly high methanol yield in CO_2 hydrogenation. From TEM (Fig. 2a), small islands of two most stable intermediate phases of Rh-In system (RhIn and RhIn₃) at the materials' interfaces were observed, suggesting that limited In reduced from In₂O₃ and decorated on exposed surfaces of Rh nanoparticle would result in a local Rh-In alloy composition.[29] Therefore, widely accepted surface bimetallic alloy models were used in our DFT calculations. Considering that the size of the majority Rh-In nanoparticles in co-RhIn/(5In5Al)O catalyst is 1-3 nm, in which the surface defects can have a profound effect toward the catalytic properties, we performed DFT calculations on a representative stepped surface, i.e., Rh(211) and two In-doped Rh(211) surfaces with 50% or 100% of the step-edge Rh sites substituted by In, denoted as RhIn(211)_a and RhIn(211)_b, respectively, to elucidate the effect of In doping (see Computational Details and Fig. S7 in the SI). In addition, to understand the superior catalytic performance of the Rh-In bimetallic catalyst to the Cu-Zn bimetallic catalyst, we also performed calculations on Cu(211) and two CuZn(211) surfaces resembling the RhIn(211) counterparts, denoted as CuZn(211)_a and CuZn(211)_b, respectively. In line with the Rh *3d* XPS and Rh K-edge XANES results (Fig. 3), Bader charge analysis (Table S4), of the surface Rh(211) with different degrees of In incorporation confirms that charge transfer from In to Rh will occur upon Rh-In alloy formation. Table 2 summarises the hydrogen adsorption energies, as well as the energy differences of surface adsorbed HCOO* and COOH* ($E_{diff} = E_{HCOO^*} - E_{COOH^*}$) on the selected model surfaces. For the Rh (211) surface, electron-donating In significantly strengthens the relative stability of HCOO*, especially for the Rh (211) surface heavily substituted by In (denoted as RhIn(211)_b) as anticipated to our bimetallic Rh-In catalyst. Interestingly, RhIn(211)_b and CuZn(211)_b surfaces have similar strongly negative E_{diff} (-1.20 eV and -1.11 eV, respectively), indicating the formation of HCOO* is energetically more favourable than that of COOH* on both bimetallic alloy cases. Behrens *et al.* have reported a similar stabilisation effect of adsorbed HCOO* by substituting Cu step sites with the electron richer Zn atoms, and this effect is essential for the direct methanol formation.[10] On the other hand, sufficient hydrogen coverage on the catalyst surface is an equally important prerequisite to partially hydrogenate the HCOO* to methanol or fully to methane in the CO_2 hydrogenation reaction. H adsorption energy (E_{ads}) was then calculated. It corresponds to the difference between the DFT energies of the H adsorbed on the model surface (adsorption complex) and the sum of the clean surface and the gas-phase H_2 molecule, from which a more negative E_{ads} indicates H species is more favorable to be adsorbed on the surface. The result in Table 2 clearly shows that H adsorption on a Cu-Zn surface is energetically favoured but much weaker than that on the Rh-In surface, indicating a lower coverage of H and hence a lower possibility of successful H_2 dissociation (activation) on Cu-Zn

compared to Rh-In. At the H_2-deficient conditions, low coverage of H would inhibit the further hydrogenation of HCOO*. Nevertheless, the formation of CO from COOH* is less dependent on the surface H coverage.[8] Therefore, although the formation of COOH* is thermodynamically less favourable to take place than that of the parallel route of HCOO*, COOH* will kinetically be rapidly consumed by converting it into CO, giving rise to the higher rate of RWGS reaction. In contrast, the Rh-based surfaces show superior ability in activating H_2 as indicated by their strongly negative H adsorption energies. In principle, this indicates that Rh and Rh-In sites can readily seize H_2 and proceed with hydrogenation of the preferentially formed HCOO* under H_2-deficient conditions. Moreover, a heavily In-doped Rh surface (i.e., RhIn(211)_b model surface and our high-performing Rh-In bimetallic catalyst) with a moderate H adsorption energy provides active sites for an efficient hydrogen utilisation with enhanced methanol selectivity/yield.

The difference of the surface adsorption properties of Rh, Rh-In, and Cu-Zn surfaces, as demonstrated in the DFT result, were then verified by the experimental surface adsorption analysis. The in-situ FTIR spectra in Fig. 4a indeed show that different forms of adsorbed CO species and formates are preferably formed on co-Rh/Al₂O₃ and co-RhIn/(5In5Al)O surfaces, respectively, whereas RWGS products (CO and H_2O) are found in Cu/ZnO/Al₂O₃ (further details are shown in Section 7 of the SI). From DFT result, it is important to have appropriate adsorptivity for both CO_2 and H_2 on the active sites for efficient conversion of the two molecules to methanol: Too strong adsorption for either molecule may cause a change in selectivity due to side reactions. According to the pulse experiment result in Fig. 4b, it confirms that co-Rh(5In5Al)O contains active adsorption sites for both CO_2 and H_2, hence giving rise to excellent methanol production. In contrast, Cu/ZnO/Al₂O₃ and In₂O₃-Al₂O₃ show a significantly lower H_2 uptake (low hydrogenation activity), therefore, the RWGS reaction becomes more dominant than the extensive CO_2 hydrogenation to methanol, leading to more CO production. On the other hand, excellent methanation activity of the co-Rh/Al₂O₃ catalyst is likely to stem from its higher intrinsic adsorption capacity of Rh to H_2 over CO_2 adsorption. These experimental surface adsorption results can explain the alteration of Rh adsorption property by the presence of In, and can also demonstrate the reason for the much lower methanol selectivity on Cu/ZnO/Al₂O₃ catalysts than the Rh-In catalyst, under low H_2/CO_2 conditions in particular.

Table 2. Calculated energy differences of surface adsorbed HCOO* and COOH* species and H adsorption energies at various surfaces.

Model surface	E_{diff}[a]	E_{ads}[b]
Rh(211)	-0.25	-0.59
RhIn(211)_a	-0.37	-0.56
RhIn(211)_b	-1.20	-0.35
Cu(211)	-0.92	-0.21
CuZn(211)_a	-0.90	-0.21
CuZn(211)_b	-1.11	-0.03

[a] E_{diff} (eV): Energy differences of surface adsorbed HCOO* and COOH* species.

[b] E_{ads} (eV): H adsorption energies
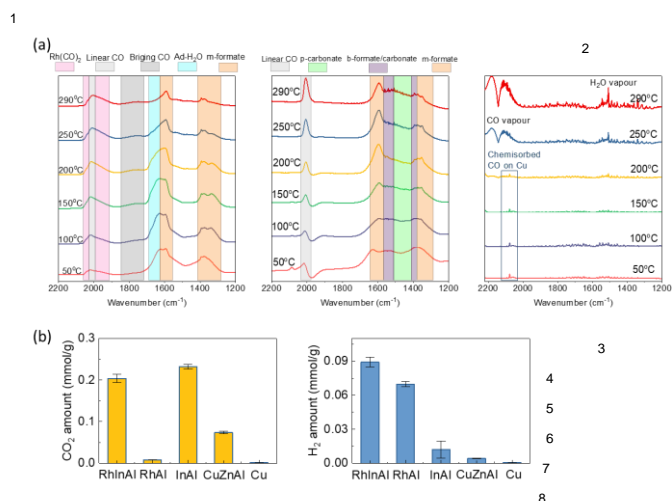
Figure 4. Surface adsorption properties.
a) In-situ FTIR spectra of the adsorbed species on the reduced catalysts. A gas flow of 25% CO_2 and 75% H_2 is passed through the catalyst pellets made by 20 mg of samples at various temperatures. b) CO_2 (left) and H_2 (right) uptakes per gram of catalyst derived from CO_2 and H_2 pulse experiments at 50 °C. RhInAl: co-RhIn/(5In5Al)O); RhAl: co-Rh/Al$_2$O$_3$; InAl: In$_2$O$_3$-Al$_2$O$_3$; CuZnAl: commercial Cu/ZnO/Al$_2$O$_3$. An unmodified Cu nanoparticles sample, which shows very poor adsorption toward both CO_2 and H_2, is presented as a comparison. Error bars indicate the standard deviation of 3 repeated data points taken for each experiment.

Conclusion

In summary, the unmodified Rh catalyst is well known to carry out extensive hydrogenation of CO_2 to methane. However, this study illustrates that the new Rh-In bimetallic catalyst offers selective sites for capturing hydrogen gas and CO_2 to approach stoichiometric methanol formation with unprecedentedly high methanol yield (up to 1 $g_{MeOH} \cdot g_{cat}^{-1} \cdot h^{-1}$) under industrially applicable flow conditions. We believe that the usage of such selective hydrogen-to-methanol catalyst may thus open a new avenue for more efficient coupling with the upstream CO_2/H_2 production from renewable biomass feedstocks. Considering the cost of Rh and In, further effort to enhance their atomic effectiveness in catalyst fabrication including core-shell design, mixed ion structure, and atom implantation is needed.

Acknowledgements

[1] J. Turner, G. Sverdrup, M. K. Mann, P.-C. Maness, B. Kroposki, M. Ghirardi, R. J. Evans, D. Blake, *Int. J. Energy Res.* **2008**, *32*, 379–407.

[2] M. Niermann, S. Drünert, M. Kaltschmitt, K. Bonhoff, *Energy Environ. Sci.* **2019**, *12*, 290–307.

[3] G. A. Olah, *Angew. Chemie Int. Ed.* **2005**, *44*, 2636–2639.

[4] R. D. Cortright, R. R. Davda, J. A. Dumesic, *Nature* **2002**, *418*, 964–967.

[5] M. Specht, A. Bandi, F. Baumgart, C. N. Murray, J. Gretz, *Greenh. Gas Control Technol.* **1999**, *723*, 1–6.

[6] X. Yin, D. Y. C. Leung, J. Chang, J. Wang, Y. Fu, C. Wu, *Energy & Fuels* **2005**, *19*, 305–310.

[7] M. Götz, J. Lefebvre, F. Mörs, A. McDaniel Koch, F. Graf, S. Bajohr, R. Reimert, T. Kolb, *Renew. Energy* **2016**, *85*, 1371–1390.

[8] F. Liao, X.-P. Wu, J. Zheng, M. M.-J. Li, A. Kroner, Z. Zeng, X. Hong, Y. Yuan, X.-Q. Gong, S. C. E. Tsang, *Green Chem.* **2017**, *19*, 270–280.

[9] F. Liao, X.-P. Wu, J. Zheng, M.-J. Li, Z. Zeng, X. Hong, A. Kroner, Y. Yuan, X.-Q. Gong, S. C. E. Tsang, *Catal. Sci. Technol.* **2016**, *6*, 7698–7702.

[10] M. Behrens, F. Studt, I. Kasatkin, S. Kühl, M. Hävecker, F. Abild-Pedersen, S. Zander, F. Girgsdies, P. Kurr, B.-L. Kniep, et al., *Science* **2012**, *336*, 893–7.

[11] S. Kuld, M. Thorhauge, H. Falsig, C. F. Elkjær, S. Helveg, I. Chorkendorff, J. Sehested, *Science* **2016**, *352*, 969–74.

[12] M. M.-J. Li, Z. Zeng, F. Liao, X. Hong, S. C. E. Tsang, *J. Catal.* **2016**, *343*, 157–167.

[13] M. Saito, *Catal. Surv. From Japan* **1998**, *2*, 175–184.

[14] A. Gotti, R. Prins, *Catal. Letters* **1996**, *37*, 143–151.

[15] H. Kusama, K. Okabe, K. Sayama, H. Arakawa, *Appl. Organomet. Chem.* **2000**, *14*, 836–840.

[16] M. S. Frei, C. Mondelli, R. García-Muelas, K. S. Kley, B. Puértolas, N. López, O. V. Safonova, J. A. Stewart, D. Curulla Ferré, J. Pérez-Ramírez, *Nat. Commun.* **2019**, *10*, 3377.

[17] B. Ouyang, W. Tan, B. Liu, *Catal. Commun.* **2017**, *95*, 36–39.

[18] F. Studt, I. Sharafutdinov, F. Abild-Pedersen, C. F. Elkjær, J. S. Hummelshøj, S. Dahl, I. Chorkendorff, J. K. Nørskov, *Nat. Chem.* **2014**, *6*, 320–324.

[19] E. M. Fiordaliso, I. Sharafutdinov, H. W. P. Carvalho, J. D. Grunwaldt, T. W. Hansen, I. Chorkendorff, J. B. Wagner, C. D. Damsgaard, *ACS Catal.* **2015**, *5*, 5827–5836.

[20] O. Martin, A. J. Martín, C. Mondelli, S. Mitchell, T. F. Segawa, R. Hauert, C. Drouilly, D. Curulla-Ferré, J. Pérez-Ramírez, *Angew. Chemie Int. Ed.* **2016**, *55*, 6261–6265.

[21] J. Wang, G. Li, Z. Li, C. Tang, Z. Feng, H. An, H. Liu, T. Liu, C. Li, *Sci. Adv.* **2017**, *3*, e1701290.

[22] M. M.-J. Li, C. Chen, T. Ayvali, H. Suo, J. Zheng, I. Teixeira, L. Ye, H. Zou, D. O'Hare, S. C. E. Tsang, *ACS Catal.* **2018**, *8*, 4390–4401.

[23] Y. Yin, B. Hu, X. Li, X. Zhou, X. Hong, G. Liu, *Appl. Catal. B Environ.* **2018**, *234*, 143–152.

[24] N. Rui, Z. Wang, K. Sun, J. Ye, Q. Ge, C. Liu, *Appl. Catal. B, Environ.* **2017**, *218*, 488–497.

[25] J. L. Snider, V. Streibel, M. A. Hubert, T. S. Choksi, E. Valle, D. C. Upham, J. Schumann, M. S. Duyar, A. Gallo, F. Abild-Pedersen, et al., *ACS Catal.* **2019**, *9*, 3399–3412.

[26] J. Graciani, K. Mudiyanselage, F. Xu, A. E. Baber, J. Evans, S. D. Senanayake, D. J. Stacchiola, P. Liu, J. Hrbek, J. Fernández Sanz, et al., *Science* **2014**, *345*, 546–50.

[27] L. Lin, S. Yao, Z. Liu, F. Zhang, N. Li, D. Vovchok, A. Martínez-Arias, R. Castañeda, J. Lin, S. D. Senanayake, et al., *J. Phys. Chem. C* **2018**, *122*, 12934–12943.

[28] S. Yang, S. H. Pang, T. P. Sulmonetti, W. Su, J. Lee, B. Hwang, C. W. Jones, *ACS Catal.* **2018**, *8*, 12056–12066.

[29] P. Anres, P. Fossati, J. P. Bros, *J. Alloys Compd.* **1998**, *266*, 241–246.

[30] J. VIS, *J. Catal.* **1985**, *95*, 333–345.

[31] G. M. Nuñez, A. J. Rouco, *J. Catal.* **1988**, *111*, 41–49.

[32] Y. Okamoto, N. Ishida, T. Imanaka, S. Teranishi, *J. Catal.* **1979**, *58*, 82–94.

[33] Z. M. Detweiler, S. M. Wulfsberg, M. G. Frith, A. B. Bocarsly, S. L Bernasek, *Surf. Sci.* **2016**, 648, 188–195.

[34] S. J. Kang, J. Baik, H.-J. Shin, *J. Inorg. Organomet. Polym. Mater.* **2013**, 23, 1519–1523.

[35] N. Iwasa, T. Mayanagi, N. Ogawa, K. Sakata, N. Takezawa, *Catal. Letters* **1998**, *54*, 119–123.

[36] J. A. Rodriguez, J. Evans, L. Feria, A. B. Vidal, P. Liu, K. Nakamura, F. Illas, *J. Catal.* **2013**, *307*, 162–169.

[37] J. A. Herron, J. Scaranto, P. Ferrin, S. Li, M. Mavrikakis, *ACS Catal.* **2014**, *4*, 4434–4445.

[38] C. Liu, T. R. Cundari, A. K. Wilson, *J. Phys. Chem. C* **2012**, *116*, 5681–5688.

[39] L. Dietz, S. Piccinin, M. Maestri, *J. Phys. Chem. C* **2015**, *119*, 4959–4966.

[40] G. C. Chinchen, P. J. Denny, J. R. Jennings, M. S. Spencer, K. C Waugh, **1988**, *Appl. Catal.* 36, 1–65.

[41] Y. F. Zhao, Y. Yang, C. A. Mims, C. H. F. Peden, J. Li, D. Mei, **2011**, *J. Catal.* 281, 199–211.

[42] S. Kattel, P. J. Ramírez, J. G. Chen, J. A. Rodriguez, P. Liu, *Science* **2017**, *355*, 1296–1299.

Entry for the Table of Contents

RESEARCH ARTICLE
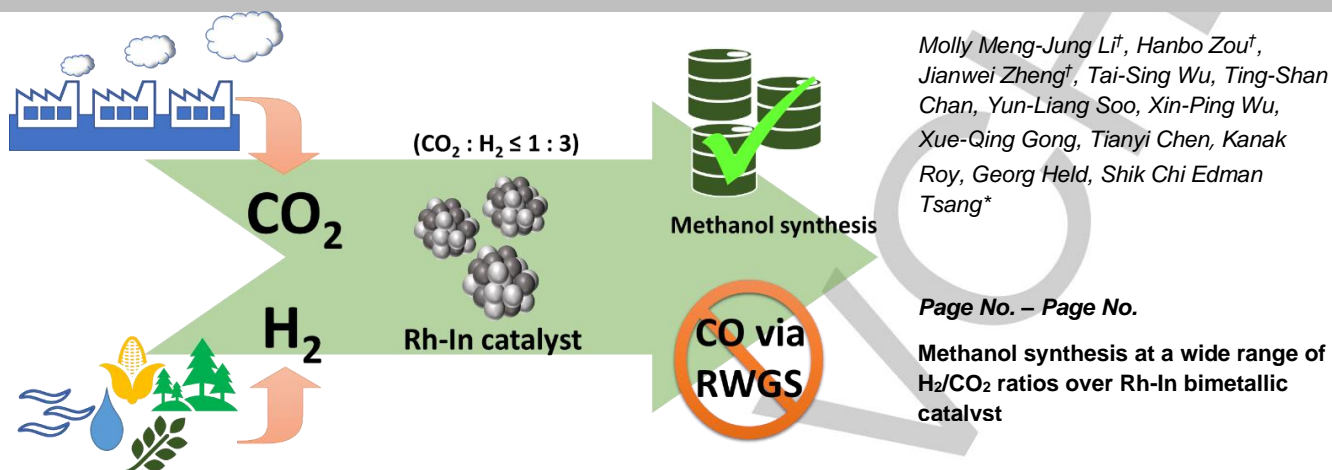
$(CO_2 : H_2 \leq 1 : 3)$

CO$_2$

H$_2$

Rh-In catalyst

Methanol synthesis

CO via RWGS

Molly Meng-Jung Li[†], Hanbo Zou[†], Jianwei Zheng[†], Tai-Sing Wu, Ting-Shan Chan, Yun-Liang Soo, Xin-Ping Wu, Xue-Qing Gong, Tianyi Chen, Kanak Roy, Georg Held, Shik Chi Edman Tsang*

Page No. – Page No.

Methanol synthesis at a wide range of H$_2$/CO$_2$ ratios over Rh-In bimetallic catalyst

Bimetallic Rh-In catalyst offers selective sites for capturing hydrogen and CO$_2$ to approach methanol formation under H$_2$-deficient feedstock compositions with high methanol yield but minimise reverse water-gas shift reaction. Using this catalyst, a convenient methanol synthesis based on renewable biomass-derived feedstocks with lower energy costs can be established.